A Pressure-shear Plate Impact Experiment for Investigating Transient Friction

by Vikas Prakash

ABSTRACT—A pressure-shear plate impact experiment is introduced to study time-resolved friction at interfaces subjected to high sliding speeds under relatively high normal pressures. The conditions of slip at the interface are varied by changing the surface roughness of the impacting plates and by varying the applied normal to shear stress ratio. The configuration offers the simplicity of allowing the interpretation of the experimental data by using the frame-work of one-dimensional plane wave analysis. The interfacial material pairs investigated in the present study are comprised of a wear-resistant grade of tungsten carbide and either an AISI 4340 steel or a Ti-6Al-4V alloy. The experimental results indicate that the coefficient of friction increases with the increase in surface roughness of the tungsten-carbide plates and with cumulative slip at the interface.

KEY WORDS—friction analysis, dynamic testing, impact analysis, interferometry, metal working, test procedures.

Introduction

In recent times much attention has been focused on the mechanics of high-speed deformation processes for increasing manufacturing productivity through reduction in actual processing times. Substantial savings have been achieved in this regard in the high-speed machining of aluminum alloys and high-speed grinding of hard composites. To fully characterize the material behavior in analytical models of deformation processes, friction effects must be incorporated. For a long time the majority of the analysis which accounted for the effect of friction was restricted to the law $\tau = \mu N$ where τ is the transmitted shear stress, N is the normal stress, and μ is the coefficient of friction. This law was first put forward by Leonard da Vinci in 1508. In 1778, Coulomb proposed a frictional law in which the coefficient of friction μ was not a constant but was pressure dependent, i.e., $\mu = \mu(p)$ for a given material interface. In 1930 Bowden and Tabor[1] measured the real contact area under a sliding interface, accounting for surface roughness and contact stresses analyzed by Hertz.[2] They established the appearance of high temperature flashes at contact points and formulated their theory of welded junctions between rubbing interfaces. At the same time, in the Soviet Union, a molecular-mechanical theory was forwarded. This theory was based on the dual nature of the friction force, which is comprised of the intermolecular interaction force between the contacting surfaces and the mechanical resistance to sliding resulting from plowing action of the asperities. In 1939, Kraglesky[3] introduced the concept of the formation of a third phase between rubbing bodies. He showed that the friction force between the rubbing bodies was controlled by this third phase and depended on the state of the surface, the pressure between the mating bodies, the contact time and the rate of application of the load.

As the knowledge of surface friction has accumulated many theories concerning the origin and evolution of slip resistance have been put forward. Although specific details differ from one theory to another, according to Suh and Sin[4] and Suh,[5] the major factors contributing to frictional resistance between sliding surfaces are the combined effects of elastic-plastic deformation and fracture of asperities, intense plastic deformation in the near surface layers of contact, adhesion of newly created surfaces, and plowing of the interface surface by hard entrapped wear particles. The relative contribution of the various mechanisms depends upon the condition of the sliding interface, their surface topography, effects of the environment, and history of sliding, Suh[5] has reviewed some micromechanical models for contributions due to asperity deformation, adhesion and plowing. These micromechanical models qualitatively explain the individual contributions to slip resistance, but at present there is no comprehensive model incorporating these micromechanisms into a predictive model for slip and its evolution. Typically they do not reflect the transient nature of friction process inherent at high sliding speeds and time varying normal pressures. Experimental observations indicate that at low sliding speeds the coefficient of friction depends on surface roughness, cleanliness, and similar factors but not on velocity. At higher velocities the situation changes: μ becomes velocity dependent, falling as the velocity increases. Experience suggests that this fall is a consequence of friction induced heating which is sufficient to cause local asperity melting. Thus, the interface sees a multistage friction process of static friction, followed by dynamic friction, and finally viscous friction in the molten layer.

To adequately understand dynamic frictional behavior at such interfaces experiments are required which simulate the local conditions of pressure, slipping velocity, surface characteristics, and temperature that occur in practice. These conditions need to be realized in a simple geometry for which the local interfacial tractions and slip velocity are readily measured so that mathematical models for the friction behavior can be developed. In the present paper a plate impact pressure-shear experiment is described to study the

Vikas Prakash (SEM Member) is Assistant Professor, Case Western Reserve University, Department of Mechanical and Aerospace Engineering, Glennan Building, Cleveland, OH 44106-7222.

Original manuscript submitted: July 20, 1994. Final manuscript received: February 17, 1995.

transient frictional response of sliding interfaces. The experimental configuration allows the calculation of critical frictional parameters such as the applied normal stress, the transmitted shear stress and the interfacial slip velocity by using the framework of one-dimensional plane wave analysis. By suitably varying the experimental parameters, extreme conditions of normal pressure (100 MPa to 3 GPa) and interfacial slip velocities (1 m/s to 30 m/s) are readily achieved by using this configuration. The results of these critical experiments will provide key information to elucidate the role of the normal pressure, the slip velocity, the surface roughness and similar factors in governing the slip resistance of the interface.

Theory

The schematic of the plate impact pressure-shear friction experiment used in the present study is shown in Fig. 1. This configuration, which is a modification of the configurations used for studying the shearing resistance of metals,[6] and lubricants,[7] involves the pressure-shear loading of a target plate with a flyer plate. Further details regarding these modifications in order to achieve the objectives of the present study are described in Ref. 8. The target and the flyer plate are chosen to represent the material pair comprising the interface. The impacting plates are flat and parallel, and inclined relative to the direction of approach. Both the flyer and the target plates are unstressed initially. The target is at rest while the flyer is carried by a moving projectile at a known velocity V. Thus, the initial normal and transverse particle velocities u_0 and v_0 of the flyer are

$$u_0 = V \cos \theta \qquad v_0 = V \sin \theta \tag{1}$$

where θ is the skew angle. A laser-interferometry technique described below is used to measure the normal and transverse particle velocity at a monitoring point on the rear surface of the target plate. The measured free-surface particle velocities are used to calculate the critical frictional parameters as described in the next section.

Wave Propagation in Specimen and Flyer

At contact, both normal and transverse components of velocity are imposed on the impact face of the target. Two stress waves propagate into the flyer and the target plate; a longitudinal wave propagating at the elastic longitudinal wave speed, c_1, and a transverse wave propagating at the elastic shear wave speed, c_2. The propagation of these waves are shown schematically in a $t - X$ diagram in Fig. 2. Solid lines indicate the longitudinal wavefronts while the dashed lines indicate the shear wavefronts. The velocity and the skew angle of the projectile are controlled such that the target plate remains elastic during the experiment. Thus one-dimensional elastic wave theory can be used in the interpretation of the experimental results. The governing equations which hold along the characteristics are

$$\begin{aligned} \sigma \pm (\rho c_1)u &= \text{constant} \quad \text{along} \ \frac{dx}{dt} = \mp c_1 \\ \tau \pm (\rho c_2)v &= \text{constant} \quad \text{along} \ \frac{dx}{dt} = \mp c_2 \end{aligned} \tag{2}$$

where σ, τ are the normal and shear stresses, u and v are the normal and transverse components of the particle velocity, ρ is the mass density of the impacting plates. The quantities (ρc_1) and (ρc_2) are longitudinal and shear impedance, respectively. The constants in both equations are obtained from applying the initial and boundary conditions. Using eq (2) the components of traction at the interface, i.e., the normal pressure and the transmitted shear stress, can be related to the measured normal and transverse free surface particle velocities, $u_{fs}(t)$ and $v_{fs}(t)$ respectively, and the shear and longitudinal impedance of the target plate,

$$\begin{aligned} \tau(t) &= \frac{1}{2}(\rho c_2)_t v_{fs}(t) \quad \text{(shear stress)} \\ \sigma(t) &= \frac{1}{2}(\rho c_1)_t u_{fs}(t) \quad \text{(normal stress)} \end{aligned} \tag{3}$$

where the subscript t denotes the properties of the target plate.

From eqs (1) and (2) the free-surface velocity of the target plate under conditions of no-slip between the flyer interface can be expressed as

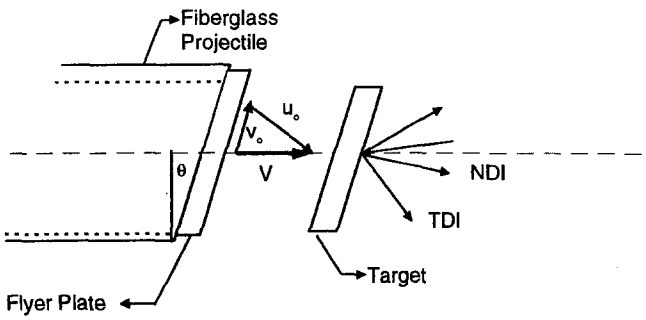

Fig. 1—Schematic of plate impact pressure-shear friction experiment

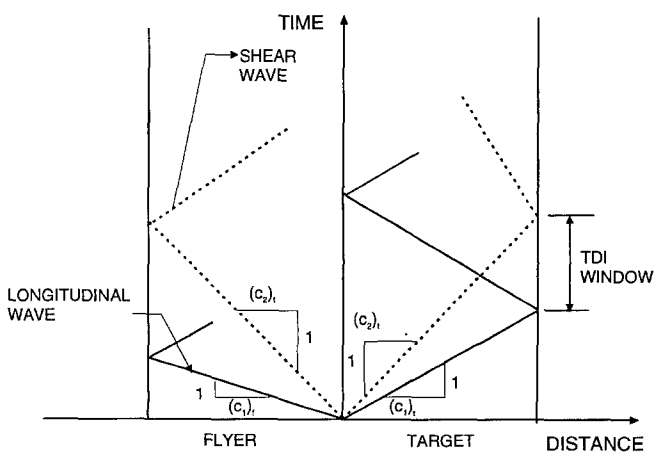

Fig. 2—Wave propagation in flyer and target

$$u_{fs} = \frac{2(\rho c_1)_f}{[(\rho c_1)_t + (\rho c_1)_b]} V \cos\theta$$
$$v_{fs} = \frac{2(\rho c_2)_f}{[(\rho c_2)_t + (\rho c_2)_f]} V \sin\theta \quad (4)$$

where the subscript f denotes the properties of the flyer material.

Based on the elementary definition of friction between two dry contact surfaces under no-slip condition, the coefficient of static friction, μ_s, satisfies

$$\mu_s \geq \frac{\tau}{\sigma} \quad (5)$$

For a fully elastic impact, with no-slip at the interface, eq (5) provides a lower bound for μ_s. When slip occurs at the flyer-target interface, the measured free surface velocity of the target plate can be used along with eq (3) to obtain the coefficient of kinetic friction, μ_K, as:

$$\mu_K(t) = \frac{\tau}{\sigma} \quad (6)$$

To calculate the interfacial slip velocity, the transverse particle velocity versus shear stress diagram is most useful. The loci of all shear stress and transverse particle velocity states for the given flyer-target plate combination is shown in Fig. 3. For a no-slip condition the state of the interface is shown by the letter A. If the interface slips at the rate V_{slip} then the transmitted shear stress at the flyer-target interface is reduced from τ_A to τ^* and the particle velocities on the flyer and the target sides of the interface are V_B and V_C, respectively. Then, the slip rate V_{slip} can be expressed in terms of the impact velocity V, the skew angle θ, the shear impedance of the flyer and the target plates and the measured free surface transverse velocity, $V_{fs}(t)$

$$V_{slip} = V_B - V_C - V \sin\theta - \left[\frac{(\rho c_2)_t + (\rho c_2)_f}{2(\rho c_2)_f}\right] V_{fs}(t) \quad (7)$$

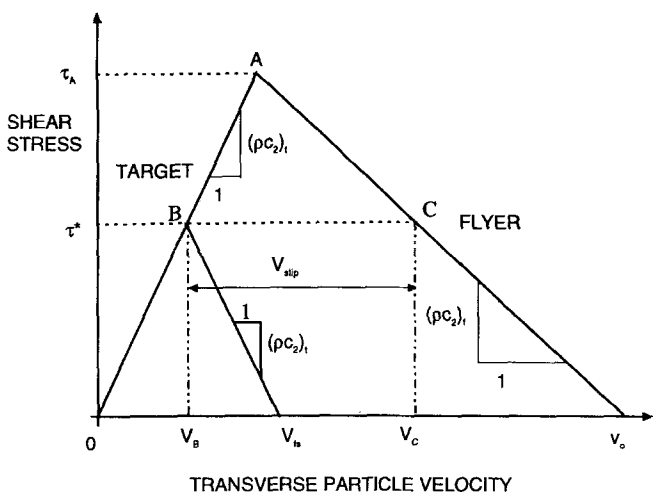

Fig. 3—Loci of all shear-stress and transverse particle velocity states at impact

Thus, by measuring the transverse and the normal particle velocities at the rear surface of the target plate and knowing the velocity of the projectile, the interfacial normal and shear tractions as well as the slip velocity can readily be obtained.

Experimental Procedure

Loading Device

The plate-impact pressure-shear friction experiments were conducted using a 63-mm bore gas gun at Brown University.[6] A fiberglass projectile carrying a flyer plate is accelerated down the gun barrel by means of compressed nitrogen gas. The rear end of the projectile holds a sealing O-ring and a plastic key which slides in the key-way in the barrel to prevent rotation of the projectile. The velocity of the projectile is measured to an accuracy of one percent or better, by recording the times at which a series of voltage biased thin wires are shorted out by contacting the flyer. The target is mounted in a chamber evacuated to a pressure of 50 μm of Hg before the shot in order to minimize the air cushion between the target and the flyer. To ensure the generation of plane waves with wavefronts sufficiently parallel to the impact face, the impacting faces are aligned parallel (within 2×10^{-5} radians), by means of an optical alignment technique.[9]

Target and Flyer Materials

The target material used for the present study is a wear-resistant grade of tungsten-carbide in a cobalt matrix, and provided by GTE. The flyer materials are AISI 4340 VAR steel (425°C temper) and commercially available Ti-6Al-4V alloy. The physical properties of these materials are given in Table 1. The tungsten-carbide plates are 40 mm in diameter and approximately 3.4 mm in thickness. These dimensions provide a useful recording time of approximately 2 μs before unloading waves from the lateral surface reach the center of the plates. Four copper pins, isolated electrically from the specimen, are placed in slots near the periphery of the impact face. The first contact of this pin with the flyer provides the triggering signal for the recording system. Moreover, these pins are used to determine the inclination between the target and flyer faces at impact. Both the specimen and the flyer are lapped flat on both sides to within 1–2 Newton's rings over the diameter. Lapping is done on a Lapmaster machine using 14.5-μm aluminum oxide powder in mineral oil for 4340 steel and Ti-6Al-4V and 15-μm boron-carbide for tungsten-carbide.

A DEKTAK surface analyzer is used to determine the surface-roughness profiles of the lapped tool and the workpiece plates. These profiles are digitally filtered to remove high frequency noise. A statistical analysis was performed on the filtered data to obtain the RMS value of the surface roughness. The surface roughness of the flyer and the target plates is varied for each experiment by polishing the specimen surfaces on Texmeth cloth using 3-μm diamond paste. This procedure allows the surface roughness of the tungsten-carbide plate to be varied from 0.02 to 0.3 μm (RMS) without losing its optical flatness. The corresponding ranges for the flyer plates are 0.05 to 0.5 μm and 0.18 to 0.67 μm for 4340 steel and Ti-6Al-4V, respectively.

TABLE 1—PHYSICAL PROPERTIES OF THE FLYER MATERIALS (4340 VAR STEEL AND Ti-6Al-4V ALLOY) AND THE TARGET (WC PLATE)

Material	Longitudinal Wave Speed c_1 mm/μs	Transverse Wave Speed c_2 mm/μs	Acoustic Impedance GPa/mm/μs	Shear Impedance GPa/mm/μs	Proportional Limit in Shear k, MPa
WC/Co	6.650	4.125	97.12	60.23	2200
AISI 4340	5.983	3.124	45.47	23.74	750
Ti-6Al-4V	6.255	3.151	27.58	13.96	450

Interferometric Technique

A laser interferometric technique is used to obtain the normal and transverse particle velocity at a central point on the rear surface of the target plates. An argon-ion laser with wavelength of 514.5 nm is used to provide a coherent monochromatic light source. Both the normal and transverse particle displacements are measured using a combined normal displacement interferometer (NDI), introduced by Barker and Hollenbach,[10] and a transverse displacement interferometer (TDI) introduced by Kim et al.[11] The optical setup is shown in Fig. 4. The NDI monitors the normal displacement of the rear surface by combining a reference beam and a beam reflected from the target such that one peak-to-peak variation of intensity of light corresponds to a displacement of $\lambda/2$. The operation of the transverse displacement interferometer is based on the phase difference between the Nth-order beams diffracted from a grating deposited on the rear surface of the target. The transverse displacement on the rear surface of the target is given by $d = n\Delta$, where $\Delta = p/2N$ is the transverse displacement corresponding to one peak-to-peak variation in intensity, p is the line spacing of the grating and n is the number of fringes recorded. In the present experiment the first-order diffracted beams from gratings have a frequency of 800–1200 lines/mm are used. To deposit the holographic gratings, one side of the target plate is polished to a mirror finish. After being cleaned, the surface is coated with a thin layer of Shipley Microposit Photo Resist S1400-17. The coated plate is then exposed to a virtual grating produced with an argon-ion laser of wavelength 514.5 nm (green light). The grating is then processed in a solution consisting of one part of Shipley Microposit Developer 303A and eight parts of fresh water. The quality of grating is checked by monitoring the diffracted beams from the grating surface.

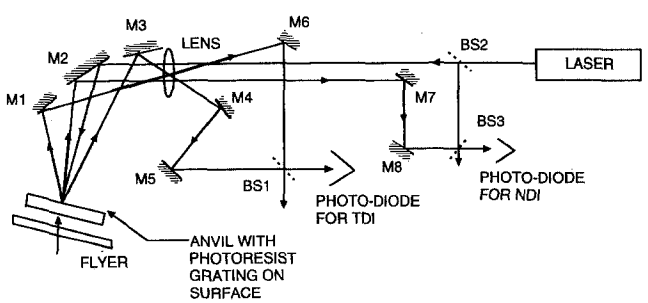

Fig. 4—Combined transverse displacement and normal displacement interferometer

Data Recording and Processing

The interference signals from the NDI and the TDI are detected by photodiodes having a rise time of approximately 1.5 ns. The output of the photodiodes is amplified by wide-band amplifiers and then recorded by LeCroy waveform digitizers having a sampling rate of 1.34 gigasamples/s, with a bandwidth of 250 MHz to 400 MHz. A typical interferometric signal obtained for pressure-shear friction experiment is shown in Fig. 5. The lower trace represents the output from the transverse displacement interferometer and the upper trace is an output from the normal displacement interferometer. A digital processing program is then used to process the recorded experimental profiles. The program first analyzes the frequency spectrum and then filters the high frequency noise by digital implementation of the fast-Fourier-transform method. The filtered data are adjusted to account for the variations in the amplitude of the fringes. After obtaining the normal and transverse displacement-time profiles, the velocity-time profiles are obtained by numerical differentiation.

Experimental Results and Discussion

A series of experiments is conducted using the pressure-shear friction experimental configuration. In all cases the tool material is tungsten carbide and the workpiece material is either 4340 steel or Ti-6Al-4V alloy. The condition of slip at the interface is varied by either altering the surface roughness of the impacting plates or by varying the skew angle of the projectile. In all cases the velocity of impact is kept low enough to prevent yielding of either of the two

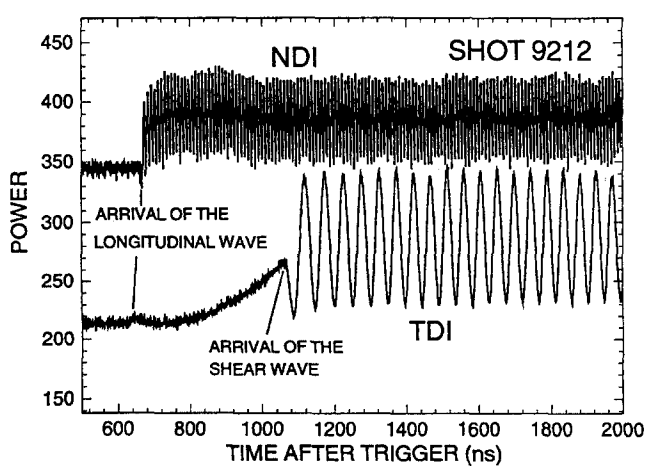

Fig. 5—Typical output of the combined transverse and normal displacement interferometer

plates. In order to ensure the validity of the plane wave analysis, measurements are restricted to the time interval (2 μs) before any unloading waves from the lateral boundaries reach the center of the plate.

A typical experimental velocity-time profile for the impact of tungsten carbide with 4340 steel is shown in Fig. 6 (Shot FRIC2). The solid line is the experimental velocity-time profile and the dash dot line represents the expected free-surface transverse velocity if no slipping occurs. The surface roughness of the tungsten carbide plate is 0.023 μm. The skew angle is 26.6 deg. The transverse velocity jumps to its no-slip elastic no-slip prediction and shows sticking for about 40 ns. Once slipping has initiated there is a tendency of the coefficient of friction to increase. The slipping velocity at the interface, calculated using eq (7), is shown along with the transmitted shear stress in Fig. 7. The average slipping speed at the interface was 11.0 m/s at a constant normal pressure of 1.34 GPa. The average value of μ_K was 0.157.

For Shot FRIC1 (Fig. 8), the surface roughness of the WC tool-plate is altered significantly in comparison to the tool-plate of Shot FRIC2. The measured RMS surface roughness of the tool-plate 0.28 μm. The skew angle is kept constant at 26.6 deg. The free-surface transverse velocity obtained in the experiment is just below the elastic prediction and the interface predicts a higher shear stress to normal stress ratio as compared to Shot FRIC2. The average slipping speeds at the interface, calculated from Fig. 9, was 4.83 m/s. The oscillations present in the transverse velocity may be due to weak interferometric signals during the later part of the experimental record. Thus by systematically changing the surface roughness of the tool material the slip condition at the interface is varied from high to relatively low slipping speeds.

Figure 10 (Shot FRIC6) and Fig. 11 (Shot FRIC7) show transverse velocity-time profiles for experiments conducted on WC/Ti-6Al-4V interfaces. The dash-dot line represents the elastic prediction based on no-slip condition and the

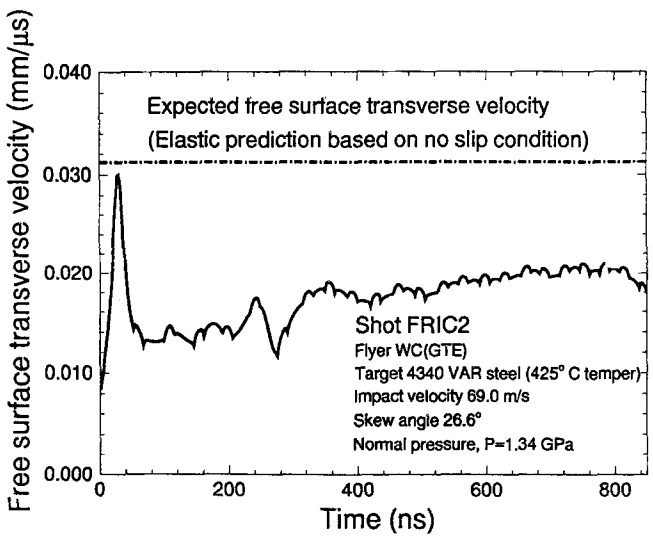

Fig. 6—Free surface transverse-velocity versus time profile for tungsten-carbide against 4340 steel (surface roughness of tungsten-carbide plate is 0.023 μm)

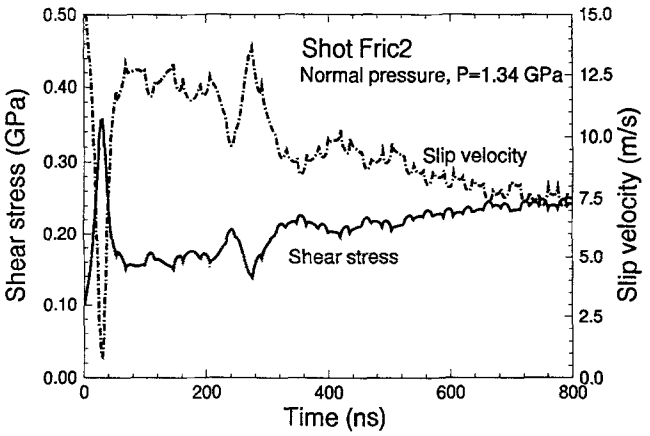

Fig. 7—Shear-stress and interfacial-slip velocity versus time for Shot FRIC2

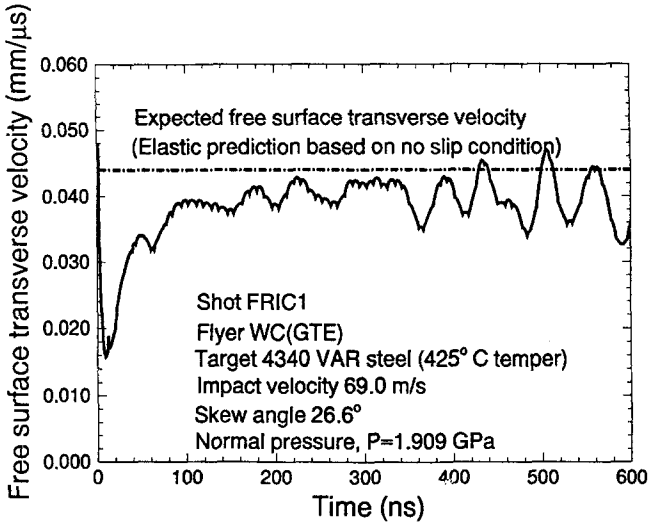

Fig. 8—Free surface transverse-velocity versus time profile for tungsten-carbide against 4340 steel (surface roughness of tungsten-carbide plate is 0.28 μm)

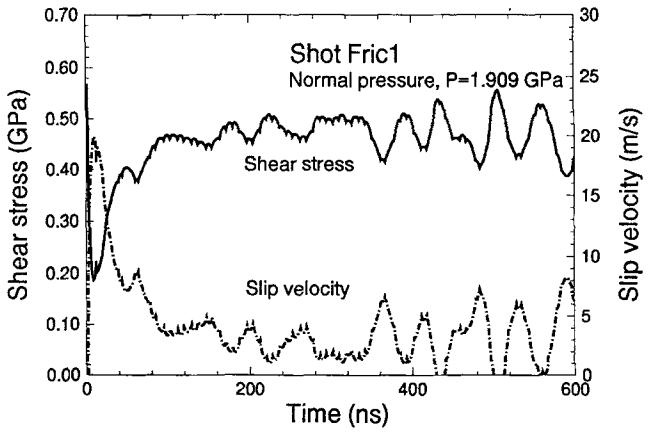

Fig. 9—Shear-stress and interfacial slip velocity versus time for Shot FRIC1

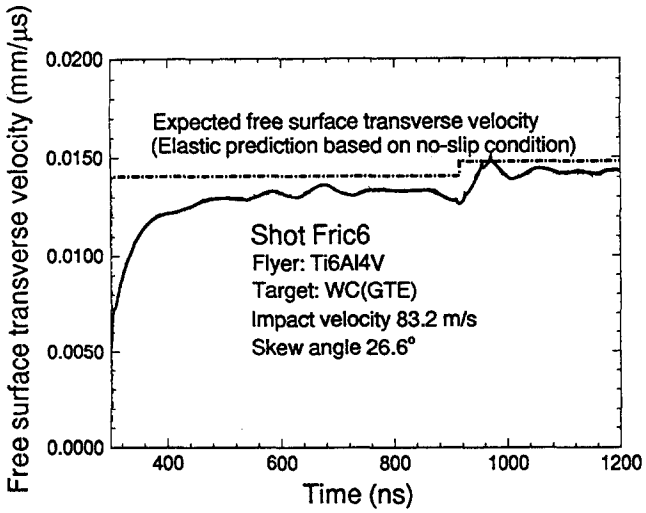

Fig. 10—Free-surface transverse velocity versus time profile for tungsten carbide against Ti-6Al-4V alloy (surface roughness of tungsten-carbide plate is 0.318 μm)

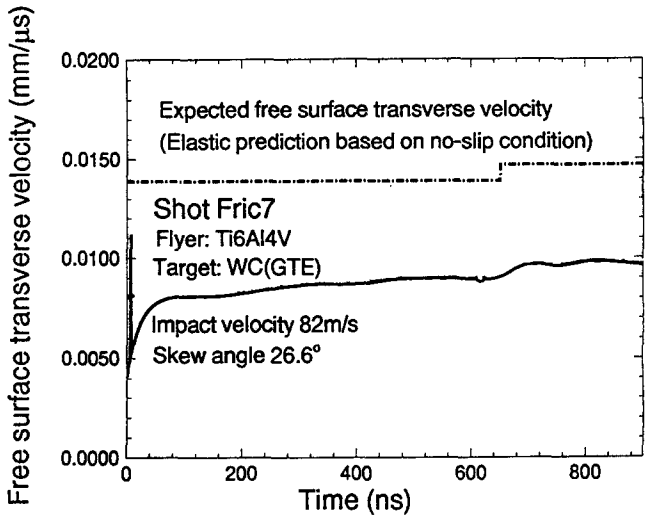

Fig. 11—Free-surface transverse velocity versus time profile for tungsten carbide against Ti-6Al-4V alloy (surface roughness of tungsten-carbide plate is 0.318 μm)

solid line represents the experimentally measured transverse velocity-time profile. The skew angle for both Shots is 26.6 deg. The RMS surface roughness of the tungsten carbide plate for shot FRIC6 is 0.318 μm whereas for shot FRIC7 is 0.042 μm. As expected, the WC/Ti-6Al-4V interface corresponding to the smoother WC (compare Fig. 12 and Fig. 13) transmits a smaller shear stress and slips at a much higher average slip speed. Moreover, in Fig. 11 and Fig. 12, after approximately 900 ns and 680 ns, respectively, a small step in the velocity-time profile is predicted. The origin of this step is due to a small tilt between the flyer and the target at impact which is generally unavoidable at low impact velocities. A complete analysis for the origin of this step and its magnitude is presented by the author in Ref 12.

Table 2 and Table 3 summarizes the experiments conducted for the present study. By systematically varying the

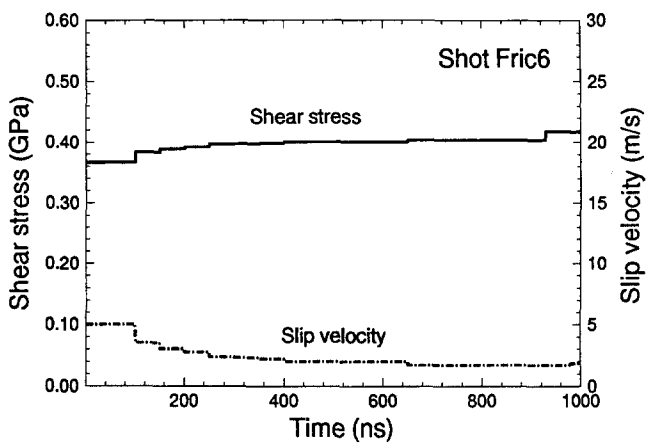

Fig. 12—Shear-stress and interfacial slip velocity versus time for Shot FRIC6

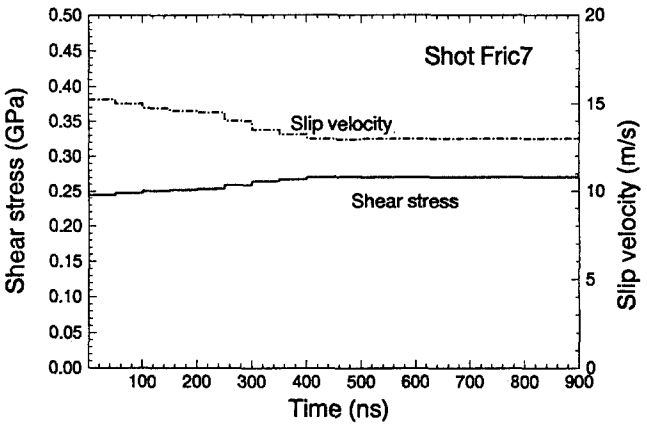

Fig. 13—Shear-stress and interfacial slip velocity versus time for Shot FRIC7

roughness of the WC tool plate, the skew angle of impact and the normal velocity, a wide range of normal pressures and interfacial slip velocities have been attained. Higher sliding speeds and hence lower values for the coefficient of kinetic friction are obtained for the case of tungsten carbide against 4340 steel. For the WC/4340 interface the coefficient of kinetic friction range from 0.132 for smooth WC plates (surface roughness RMS 0.02 μm) to as high as 0.25 for relatively rough surface (surface roughness RMS 0.285 μm). For WC/Ti-6Al-4V interface the value of μ_K ranges from 0.168 for a WC plate having a surface roughness of 0.042 μm to as high as 0.255 for a WC plate having a surface roughness of 0.318 μm. Further the slip character of the interface is determined primarily by the surface roughness of the harder tungsten carbide plate. Figure 14 shows a plot of the coefficient of kinetic friction as a function of surface roughness of the tungsten carbide plate for both the WC/4340-steel and WC/Ti-6Al-4V interfaces. The solid symbols represents the μ_K values for Ti-6Al-4V and the open symbols represent the values for 4340 steel. The coefficient of kinetic friction for both interfaces increases with the surface roughness of WC plate. Also, for a given surface roughness of the tungsten-carbide plate the

TABLE 2—SUMMARY OF EXPERIMENTS CONDUCTED ON TUNGSTEN-CARBIDE/4340 STEEL PAIR

Shot #	Skew Angle θ	Impact Velocity m/s	Normal Stress MPa	WC Roughness RMS (μm)	4340 Steel Roughness RMS (μm)	Average Slip Rate (m/s)	μ_k	$\mu_s \geq$
FRIC1	26.6 deg	69.0	1910	0.280	0.510	6.83	0.223	—
FRIC2	26.6 deg	48.6	1340	0.023	0.067	12.0*	0.157	—
FRIC3	26.6 deg	62.1	1718	0.053	0.104	14.39	0.148	—
FRIC5	22.0 deg	70.5	2010	0.280	0.466	2.90	0.233	—
FRIC8	26.6 deg	73.9	2046	0.020	0.083	17.43	0.132	—
FRIC9	26.6 deg	86.1	2384	0.203	0.210	7.73	0.221	—
FRIC11	18.0 deg	109	3210	0.275	0.482	—	—	0.178
FRIC12	14.0 deg	114	3425	0.298	0.483	—	—	0.137
FRIC13	15.0 deg	108	3230	0.298	0.510	—	—	0.147
9208	16.0 deg	79.5	2352	0.321	0.450	—	—	0.15
9210	26.6 deg	109	3058	0.285	0.345	6.0	0.25	—
9211	30.0 deg	92.1	2520	0.240	0.323	17.0	0.21	—

*No slip initially

TABLE 3—SUMMARY OF EXPERIMENTS CONDUCTED ON TUNGSTEN-CARBIDE/Ti-6Al-4V ALLOY PAIR

Shot #	Skew Angle θ	Impact Velocity m/s	Normal Stress MPa	WC Roughness RMS (μm)	4340 Steel Roughness RMS (μm)	Average Slip Rate (m/s)	μ_k	$\mu_s \geq$
FRIC4	26.6 deg	89.2	1715	0.121	0.466	6.17*	0.232	—
FRIC6	26.6 deg	83.2	1590	0.318	0.669	1.35*	0.255	—
FRIC7	26.6 deg	82.1	1576	0.042	0.185	12.93	0.168	—
FRIC10	26.6 deg	82.0	1575	0.210	0.485	1.38	0.250	—
9205	18.0 deg	110	2226	0.310	0.521	—	—	0.170
9206	22.0 deg	108	2150	0.263	0.525	—	—	0.212
9207	25.0 deg	104	2020	0.291	0.552	—	—	0.245
9212	30.0 deg	97.5	1820	0.141	0.452	11.2	0.22	—

*No slip initially

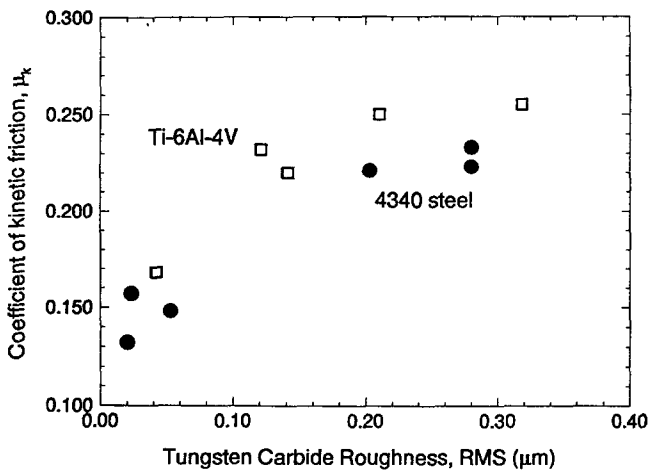

Fig. 14—Coefficient of kinetic friction as a function of the surface roughness of tungsten-carbide tool plate

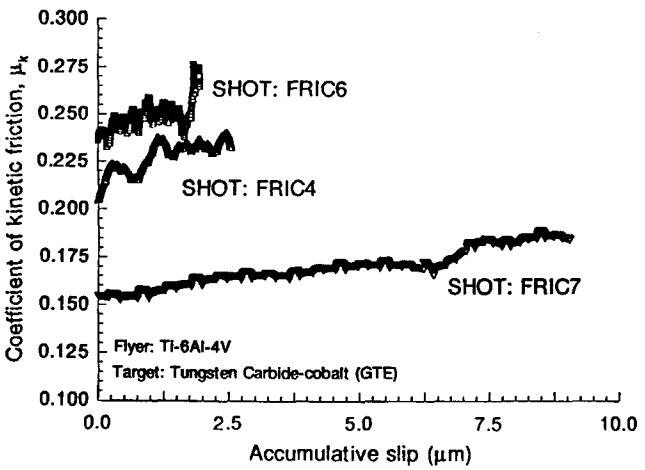

Fig. 15—Coefficient of kinetic friction as a function of cumulative slip (for tungsten-carbide/Ti-6Al-4V interface)

coefficient of kinetic friction is higher for Ti-6Al-4V than for 4340 steel. Also, for both 4340 VAR steel and Ti-6Al-4V the coefficient of kinetic-friction increases with cumulative slip as shown in Fig. 15 for Ti-6Al-4V alloy.

The μ_K values obtained in the present pressure-shear friction experiments are substantially lower than those obtained for the same combination of interface materials under quasistatic loading conditions. typical values for the coefficient of kinetic friction for WC/4340 steel and WC/Ti-6Al-4V under quasistatic loading conditions are 0.48 and 0.57,[13] respectively. In the present experiments the combined effects of the high normal pressure and high sliding speeds

generate substantial heat at the interface.[14] This heat thermally softens the interfacial layers and reduces its shear strength. This may be one reason for low μ_K values obtained in the experiments. Experimental results from rifle-bore experiments[15] have indicated that the coefficient of kinetic friction drops dramatically as a function of sliding speeds. In a particular rifle-bore experiment, the values of μ_K obtained under conditions of very low slip speeds was 0.3, but as the slip velocity was increased to 85 m/s the values of μ_K fell to 0.07.

Another reason for the lower values of μ_K may be the following: The shearing resistance of the interface under sliding conditions comprises of combined effects of adhesion between the flat surfaces, plowing by wear particles and hard surface asperities and asperity deformation. For a particular interface it is the relative contribution of these components which is responsible for the effective μ_K. In the present plate impact experiments the slipping speeds are high but the time of slip is restricted to approximately 2 μs. This allows a maximum slip of 20–30 μm during the available window time. This relatively small slip rules out any significant contribution to interfacial slip resistance from wear at the interface. Since it has been postulated by many researchers that almost half the contribution to slip resistance evolves from debris formation and plowing during the slip process, it is not surprising that the values of μ_K obtained in the present experiments are much lower.

Conclusions

A plate impact pressure-shear friction experiment is introduced to study time-resolved frictional characteristics at interfaces sliding at 1–30 m/s under relatively high normal pressures (500 MPa to 3 GPa). The experimental configuration allows the interpretation of experimental data by means of one-dimensional plane-wave analysis. Preliminary experiments on WC/4340 steel and WC/Ti-6Al-4V alloy interfaces have shown the feasibility of using the experiment for investigating interfacial friction. The experimental results indicate that the sliding resistance for both WC/4340 steel and WC/Ti-6Al-4V interfaces with the increase in surface roughness of tungsten-carbide plates and with cumulative slip at the interface.

Acknowledgment

The author would like to acknowledge the assistance of Professor Rodney J. Clifton at Brown University in carrying out this research. Partial support and the tungsten carbide plates were provided by GTE.

References

1. Bowden, F.P. and Tabor, D. "The Area of Contact Between Stationary and Moving Surfaces," Proc. Roy. Soc., **169** *(N938), 391–413 (1939).*

2. Hertz, H., "Uber die Beruhrung fester elastischer Korper," J. Reine and Angewandte Mathematik, **91,** *156–171 (1882).*

3. Kragelsky, I.V., "Friction of Unlubricated Surfaces," All Union Conference on Friction and Wear of Machines, **1,** *Acad. Sci. USSR, Moscow, 543–561 (1939).*

4. Suh, N.P. and Sin, H.C., "The Genesis of Friction," Wear, **69,** *91–114 (1981).*

5. Suh, N.P., Tribophysics, Prentice Hall, Engelwood Cliffs, NJ (1986).

6. Clifton, R.J. and Klopp, R.W., "Pressure-Shear Plate Impact Testing," Metals Handbook, 9th Ed., ASM Int., Metals Park, OH, **8,** *230–239 (1985).*

7. Ramesh, K.T. and Clifton, R.J., "A Pressure-Shear Plate Impact Experiment to Study the Rheology of lubricants at High Pressures and Shearing Rates," J. Tribology, **109,** *215–222 (1987).*

8. Prakash, V., "Plate-Impact Investigations of Dynamic Fracture Initiation and Time Resolved Friction," PhD Diss., Brown Univ. (1993).

9. Kumar, P. and Clifton, R.J., "Optical Alignment of Impact Faces for Plate Impact Experiments," J. Appl. Physics, **48,** *1366–1367 (1977).*

10. Barker, L. and Hollenbach, R.E., "Interferometer Technique for Measuring the Dynamic Mechanical Properties of Materials," Rev. of Sci. Instr., **36,** *1617–1620 (1965).*

11. Kim, K.S., Clifton, R.J. and Kumar, P., "A Combined Normal and Transverse Interferometer with an Application to Impact of Y-cut Quartz," J. Appl. Physics, **48,** *4132–4139 (1977).*

12. Prakash, V. and Clifton, R.J., "Time Resolved Dynamic Friction Measurements in Pressure Shear," **AMD 165,** *Experimental Techniques in the Dynamics of Deformable Solids, ed. K.T. Ramesh, 33–48 (1993).*

13. Bhushan, B. and Gupta, B.K., Handbook of Tribology: Material Coatings and Surface Treatments, McGraw Hill Inc. (1991).

14. Irfan, M. and Prakash, V., "Contact Temperature During Sliding in Pressure Shear Impact," Proc. 1994 SEM Spring Conf., 173–182 (1994).

15. Friction Wear and Lubrication, Tribology Handbook, **1,** *ed. V. Kragelsky, Mir Publishers Moscow, Pergamon Press (1981).*